Original Paper

Audiology & Neurotology

Audiol Neurotol 2006;11:113–122
DOI: 10.1159/000090684

Published online: January 17, 2006

An Electronic Prosthesis Mimicking the Dynamic Vestibular Function

Andrei M. Shkel[a, b] Fan-Gang Zeng[b, c]

Departments of [a]Mechanical and Aerospace Engineering, [b]Biomedical Engineering, and [c]Otolaryngology – Head and Neck Surgery, University of California, Irvine, Calif., USA

Key Words
Unilateral vestibular prosthesis · Microelectromechanical system gyroscope · Vestibular dysfunction

Abstract
This paper presents a functional architecture, system level design, and electronic evaluation of a unilateral vestibular prosthesis. The sensing unit of the prosthesis is a custom-designed one-axis microelectromechanical system (MEMS) gyroscope. Similar to the natural semicircular canal, the MEMS gyroscope senses angular motion of the head and generates voltages proportional to the corresponding angular acceleration. The voltage is then converted into electric current pulses according to the physiological data relating angular acceleration to the spike count in the vestibular nerve. The current pulses can be delivered to stimulate the corresponding vestibular nerve branch. Electronic properties of the vestibular prosthesis prototype have been systematically evaluated and found to meet the design specifications. A unique feature of the present vestibular implant prototype is the scalability: the sensing unit, pulse generator, and the current source can be potentially implemented on a single chip using integrated MEMS technology.

Introduction

As the most successful neural prosthesis, cochlear implants stimulate the auditory nerve and have restored partial hearing to 100,000 deaf people [Zeng, 2004]. Using similar principles, several prostheses are being investigated to restore other senses. For example, retinal implants stimulate the optic nerve to restore vision in blind people [Weiland et al., 2005]. Vestibular implants may improve balance and spatial orientation in patients suffering from peripheral vestibular disorders [Gong and Merfeld, 2002; Rubinstein and Della Santina, 2002; Wall et al., 2002].

Diminished vestibular function, causing dizziness and balance problems, poses a serious health risk, particularly in the elderly population. Several noninvasive approaches have been taken to control dizziness and imbalance, including regular exercise, appropriate use of drugs, and sensory substitution using auditory, tactile, and visual feedback [Gauchard et al., 2003; Minor, 1999; Patla, 2003]. Alternatively, a vestibular prosthesis might be used to restore vestibular function. Merfeld and his colleagues have designed a unilateral horizontal semicircular canal prosthesis and successfully used it to stimulate the vestibular nerve in a squirrel monkey model [Gong and Merfeld, 2000, 2002; Lewis et al., 2002]. Their implementation used an off-the-shelf single axis piezoelectric vibrating gyroscope to measure the head rotation and a microcontroller to convert rotational information into elec-

KARGER

Fax +41 61 306 12 34
E-Mail karger@karger.ch
www.karger.com

Accessible online at:
www.karger.com/aud

Andrei M. Shkel
Department of Mechanical and Aerospace Engineering
University of California
Irvine, CA 92697-1275 (USA)
Tel. +1 949 824 3843, Fax +1 949 824 8585, E-Mail ashkel@uci.edu

trical pulses for direct stimulation of the vestibular nerve. Della Santina et al. [2005] recently described a multichannel vestibular prosthesis employing commercial off-the-shelf microelectromechanical system (MEMS) gyro transducers and demonstrated responses to prosthetic stimulation in vestibular-deficient animals.

Here we describe development of a MEMS-based, vestibular prosthesis prototype. The core technology is a customized silicon chip that is 5 × 5 mm in size and includes three gyroscopes and three linear and angular accelerometers [Shkel and Howe, 2002]. We envision using the MEMS gyroscope as the input and then to adapt the cochlear implant technology for signal processing and electric stimulation. The combined MEMS and integrated circuit technologies should significantly shrink the sensor size, reduce the fabrication cost, and integrate the sensing-processing-stimulating functions on the same silicon chip for a 'balance on-a-chip' system.

We first briefly summarize the function and structure of the vestibular system. We then describe the system level design and functional blocks of the proposed vestibular prosthesis. Third, we present an engineered prototype of a unilateral vestibular prosthesis and compare the prototype performance to the physiological data recorded in the vestibular nerve of squirrel monkeys. Finally, we discuss both the opportunities and challenges facing the development of a totally implantable vestibular prosthesis.

Vestibular Function and Structure

The vestibular system is responsible for maintaining balance and spatial orientation while allowing the head and body to move freely [Goldberg and Fernandez, 1975; Highstein et al., 2005; Minor, 1998]. The vestibular system accurately senses and processes position and motion information. The brain then acts on the information by using the vestibulo-ocular reflex to stabilize gaze and the vestibulo-spinal reflex to control posture and balance. The sensing unit of the vestibular system consists of three semicircular canals and two otolith organs. The three semicircular canals are orthogonal to each other and can detect rotational movements of the head by sensing angular acceleration. The two otolith organs are the saccule and utricle that detect linear movements of the head, with the saccule being sensitive to gravity and the utricle being sensitive to linear accelerations in all planes.

All vestibular organs have small sensory hair cells, which convert motion into action potentials in the vestibular nerve. Each hair cell has a resting potential and its associated nerve has a spontaneous firing rate. The mean spontaneous rate is 91 spikes/s (SD = 36) in the squirrel monkey [Goldberg and Fernandez, 1971]. The firing rate increases when a semicircular canal responds to rotation in one direction, and decreases in the other direction. The firing rate changes in the opposite direction for vestibular nerve fibers innervating the contralateral semicircular canal in the same plane. Adaptation and small nonlinearities also occur in response to constant angular acceleration [Fernandez and Goldberg, 1971]. The average sensitivity is 0.3–0.7 spike/s, per 1°/s in rats and guinea pigs [Curthoys, 1982].

The perceptual threshold for rotation detection in humans has been measured to be between 0.1°/s and 2°/s [Benson et al., 1989]. Montandon [1954] found that the acceleration threshold is $1°/s^2$ in normal healthy individuals, but greater than $6°/s^2$ in patients with vestibular dysfunction. It should be noted that the perceptual threshold is likely to be different for different rates of acceleration and highly dependent upon individuals. Nevertheless, these reported electrophysiological and behavioral data have formed the basis on which the sensing and pulse generating units are built in the proposed vestibular prosthesis.

System Design

We initially focus on a semicircular canal prosthesis to restore rotational sensibility. The prosthesis should sense motion with sufficient precision and deliver electric stimulation to the central nervous system that mimics the dynamic vestibular function. Figure 1a contrasts the natural and prosthetic systems, with both having three main functional units – a sensing unit, a pulse generator, and a stimulator. Figure 1b shows a functional block diagram for the circuit components of a vestibular prosthesis [Liu et al., 2003]. The sensing unit includes a gyroscope, a low-pass filter and a differentiator. The input is rotational motion while the output is an analog voltage that is proportional to angular acceleration along the sensing axis. The pulse generator consists of a transfer function unit and a voltage-to-frequency converter. It generates monophasic voltage pulses based on a mathematical model describing biomechanics of the vestibular organ. The current source converts the monophasic voltage pulses into biphasic, charge-balanced, cathodic-first, current pulses that can be used to safely stimulate the vestibular nerve.

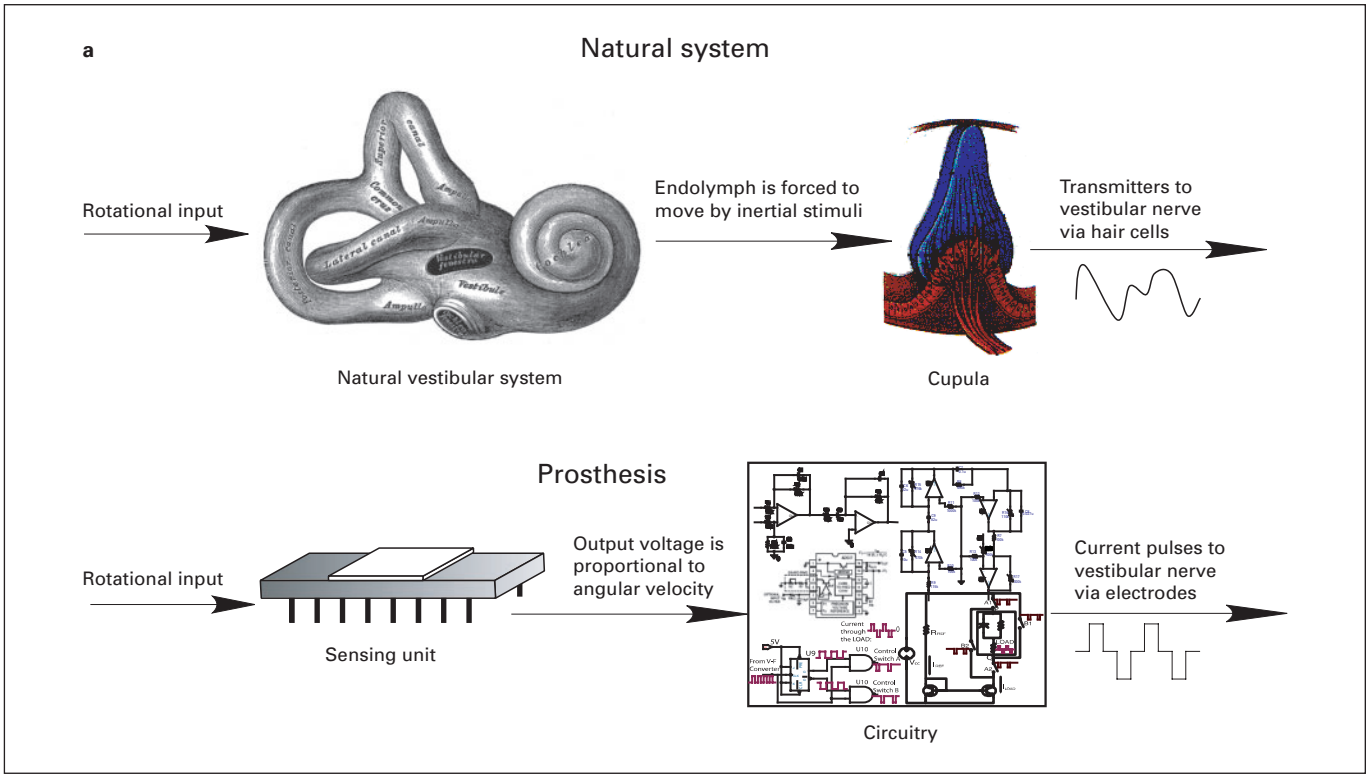

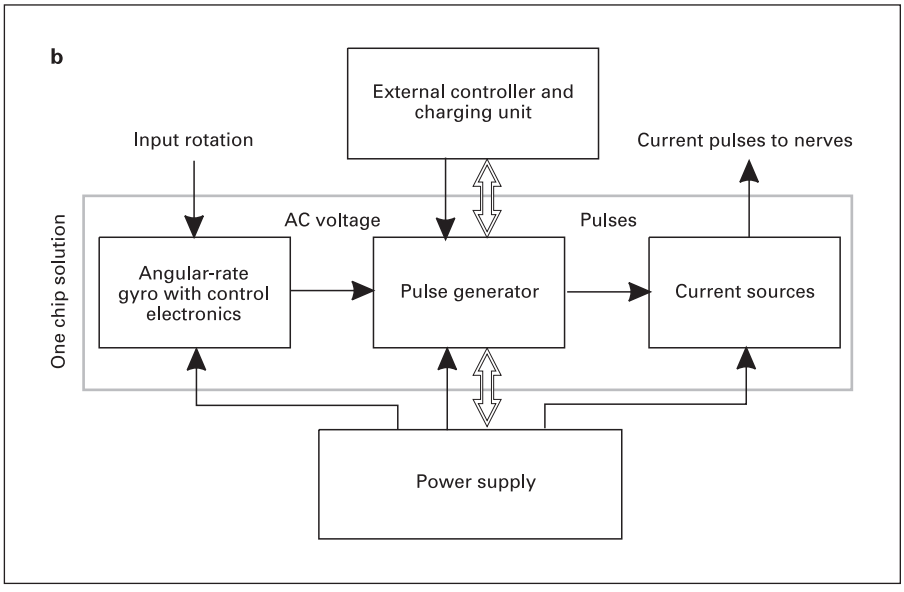

Fig. 1. a Comparison of the natural and prosthetic vestibular systems. **b** The functional block diagram of a MEMS-based vestibular prosthesis mimicking the dynamic function of the natural vestibular system.

Sensing Unit

The prosthesis utilizes a custom-made single-axis MEMS gyroscope, developed by UCI Microsystems Laboratory [Shkel, 2001]. Figure 2 shows a scanning electron micrograph of a MEMS gyroscope prototype. The gyroscope is approximately 2 × 2 mm^2 in size with a minimum feature of 5 μm. The MEMS gyroscope consumes ~10 mW power, which compares favorably with ~30 mW/rotational axis for the piezoelectric and MEMS sensors by Murata and Analog Devices Inc., respectively.

The micromachined gyroscope uses a vibrating element to measure rotational velocity based on the Coriolis

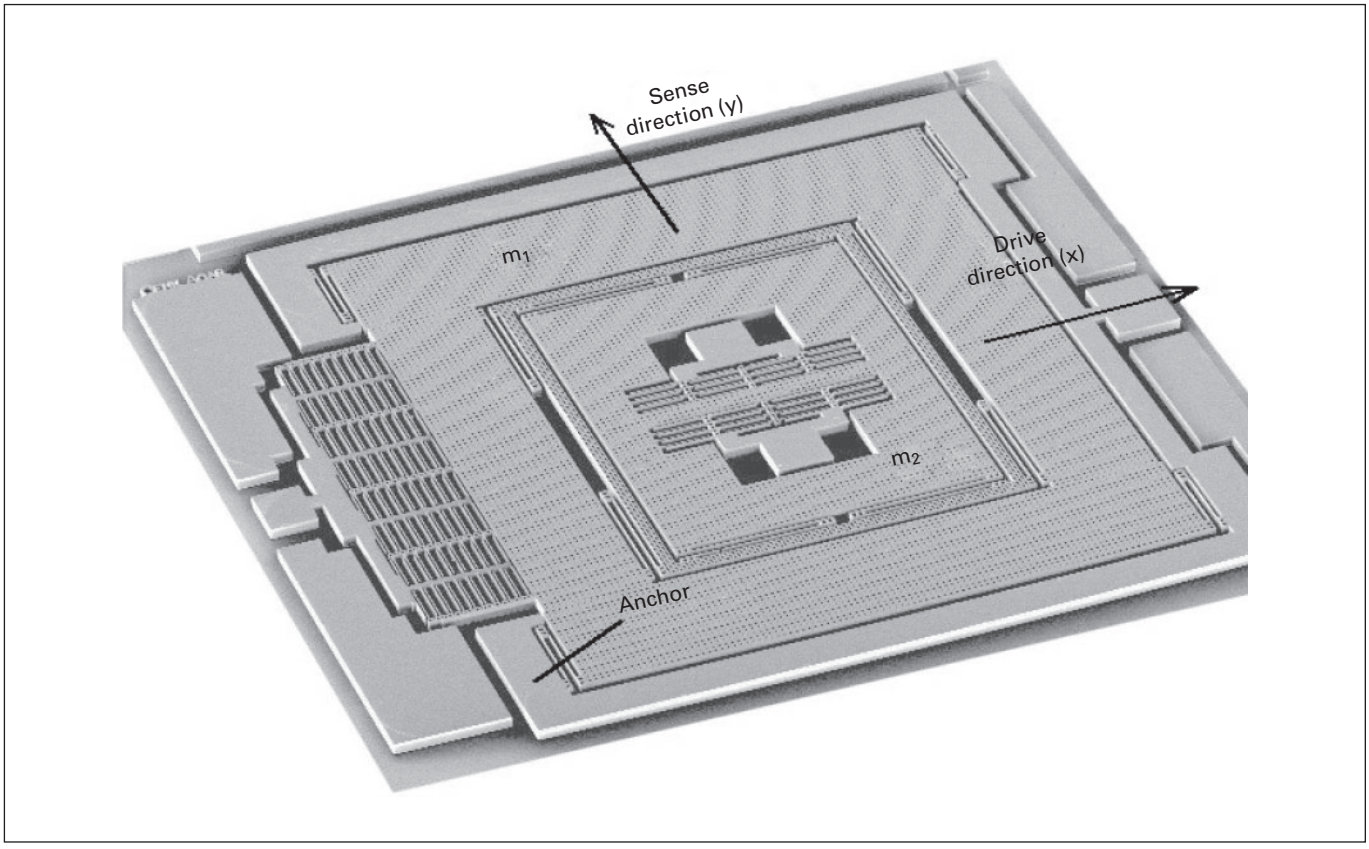

Fig. 2. Scanning electron micrograph of a prototype MEMS gyroscope.

principle [Greiff et al., 1991; Shkel et al., 2005]. The proof mass, which constitutes the active portion of the sensor, is driven by an oscillator circuit at a precise amplitude, X_D, and a relatively high frequency, ω_n, so that $x(t) = X_D \sin(\omega_n t)$. When subject to a rotation with angular velocity Ω, the proof mass will be subject to the Coriolis force. The resultant Coriolis force is perpendicular to both the input rate and the instantaneous radial velocity in the drive direction. This force produces a motion of the proof mass, $y(t)$, in a direction perpendicular to its initial oscillation:

$$\| y(t) \| = \frac{2X_D \Omega Q}{\omega_n} \quad (1)$$

This equation shows that the output deflection is proportional to the input angular velocity. The gyroscope response is also directly proportional to quality factor Q (i.e., the sharpness of the resonance) of the device. To improve performance of the MEMS gyroscope, the device has to be vacuum packaged to achieve high-amplitude response in the sensing direction. Detection of the Coriolis response is also challenging, requiring measurements of picometer scale oscillations in the sense mode, with the proof mass oscillating with tens of micrometers amplitude in the drive mode. The synchronous demodulation technique is commonly used to tackle this problem. A high-frequency carrier signal is imposed on the structure. An array of differential capacitors is used to detect picometer scale deflections due to the Coriolis-induced motion. The difference of the outputs of the differential amplifiers is amplitude demodulated at the carrier signal frequency, yielding the Coriolis response signal at the driving frequency.

We have also developed alternative vibratory gyroscopes with rate-integrating capabilities [Shkel et al., 2005]. Here we consider the design principle and specifications for a single-axis MEMS gyroscope employing a unique architecture that comprises a drive mode oscillator and a sense mode oscillator. This architecture improves sensitivity while maintaining robust operation

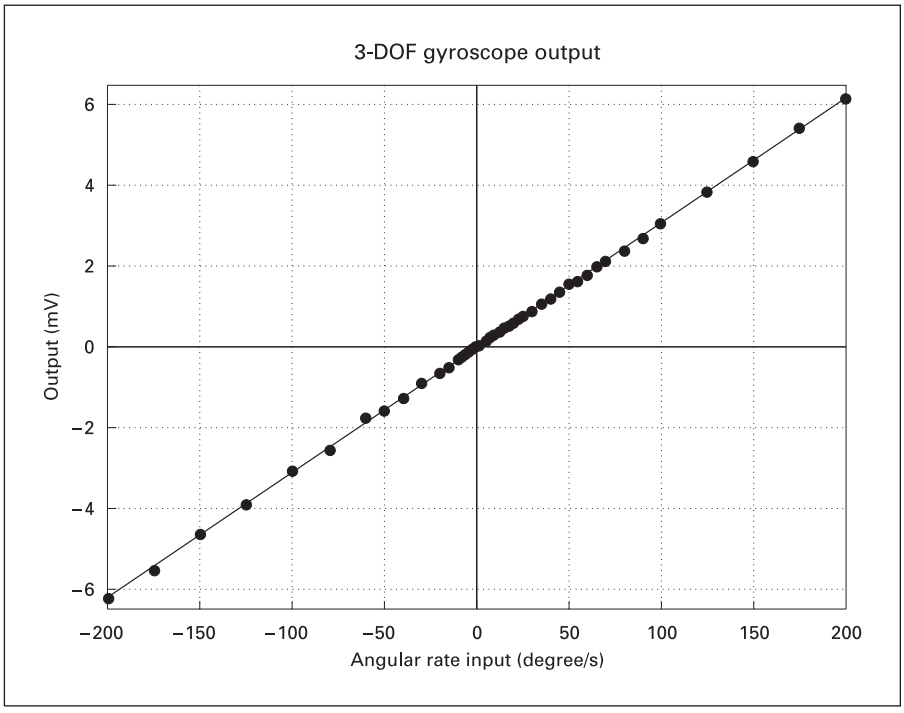

Fig. 3. A MEMS gyroscope's voltage output as a function of angular rate input.

characteristics. The device operates in air and does not require vacuum packaging. Figure 3 shows this MEMS gyroscope's linear response in DC voltage as a function of the angular rate input. The gyroscope has a sensitivity of 0.0694 mV/degree/s and a noise floor of 0.211 mV/$\sqrt{}$Hz at a 50-Hz bandwidth, yielding a resolution of 3.05°/s/$\sqrt{}$Hz at the same bandwidth.

The MEMS gyroscope can sense any type of angular rotation (constant or nonconstant rotational rate), while the natural vestibular organ only responds to the angular acceleration. To mimic the natural organ, a circuit differentiates the output voltage of the gyroscopes to produce a signal proportional to the angular acceleration. To minimize the effect of high-frequency noise without affecting the input motion signal, which is usually less than 10 Hz, a 3030-Hz low-pass filter is used prior to the differentiator [Liu et al., 2003].

Pulse Generator

The pulse generator consists of a transfer function unit emulating the dynamics of the natural vestibular organ. It uses a high-order transfer function, described by two zeros and three poles, to encode angular acceleration by increasing or decreasing the firing rate from the spontaneous rate of the vestibular nerve. The transfer function is modeled as a linear torsion-pendulum system [Steinhausen, 1931; von Egmond et al., 1949]. In this model, the cupula and endolymph are treated as a heavily damped, second-order linear system, where the cupula angular deflection $\varepsilon(t)$ is related to angular acceleration $\alpha(t)$ by the following differential equation:

$$\Theta\frac{d^2\varepsilon(t)}{d^2t}+\Pi\frac{d\varepsilon(t)}{dt}+\Delta\varepsilon(t)=\Theta\alpha(t) \quad (2)$$

where $\tau_1 = \Pi/\Delta$ and $\tau_2 = \Theta/\Pi$ are two time constants defined by morphology and material properties of the vestibular end-organ [Groen, 1956].

Furthermore, the relationship between the input angular acceleration and the overall change in firing rate of neurons is described by:

$$H(s)=\frac{\tau_A s}{1+\tau_A s}\frac{1+\tau_L s}{(1+\tau_1 s)(1+\tau_2 s)} \quad (3)$$

where τ_1 and τ_2 are time constants of the pendulum model described above, τ_A is related to the level of neuron adaptability, and τ_L is the dynamical-electrical time constants. Fernandez and Goldberg [1971] estimated: τ_1 = 5.7 s, τ_2 = 0.003 s, τ_A = 80 s, and τ_L = 0.049 s.

We use three operational amplifiers in serial to implement the transfer function relating the input angular acceleration to the firing rate of the vestibular nerve fibers. The input to the pulse generator is the voltage signal cor-

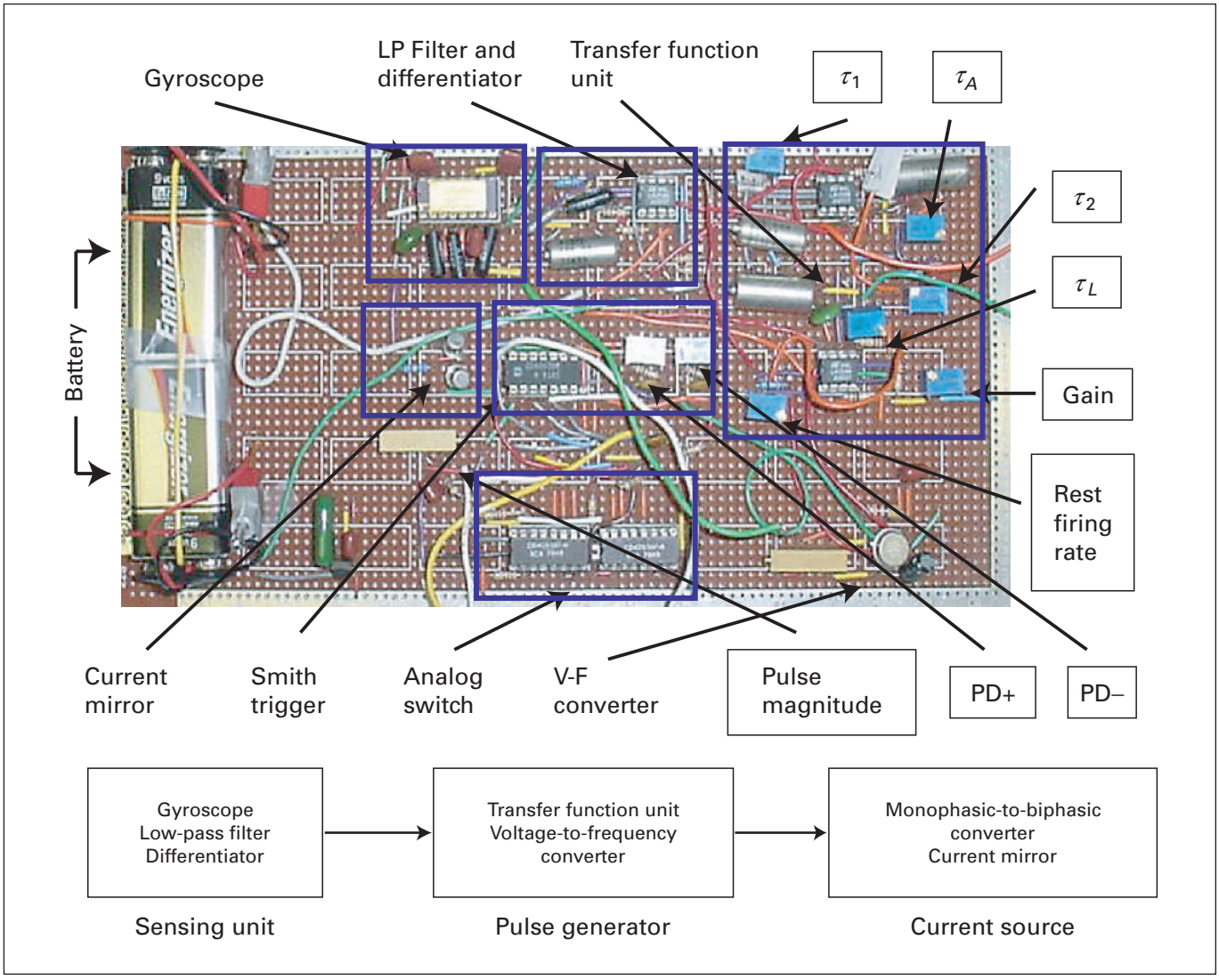

Fig. 4. A printed circuit board prototype of the electronic unilateral semicircular canal prosthesis. The dimension is ~12 × 24 cm^2.

responding to angular acceleration, and the output is the pulse train with its rate being equal to the firing rate estimated from the animal model.

Current Source

To provide effective and safe electric stimulation, the monophasic voltage signal has to be converted into a biphasic current signal [McCreery et al., 1990; Scheiner et al., 1990]. Similar to cochlear implants, the vestibular implant will likely have great individual variability in threshold and dynamic range [Zeng and Galvin, 1999]. Therefore, the electric parameters, including pulse rate, pulse amplitude, and pulse duration, have to be dynamically and individually adjusted. In our implementation, the shortest pulse duration is set at 1 ms. Therefore, the maximum rate can be set close to 500 Hz, doubling the maximum rate of 250 Hz used in a previous study [Gong and Merfeld, 2002].

Printed Circuit Board Prototype

Figure 4 shows such a vestibular prosthesis prototype implemented in a printed circuit board. The sensing unit is a z-axis gyroscope, followed by a low-pass filter and a differentiator. The pulse generator includes a transfer

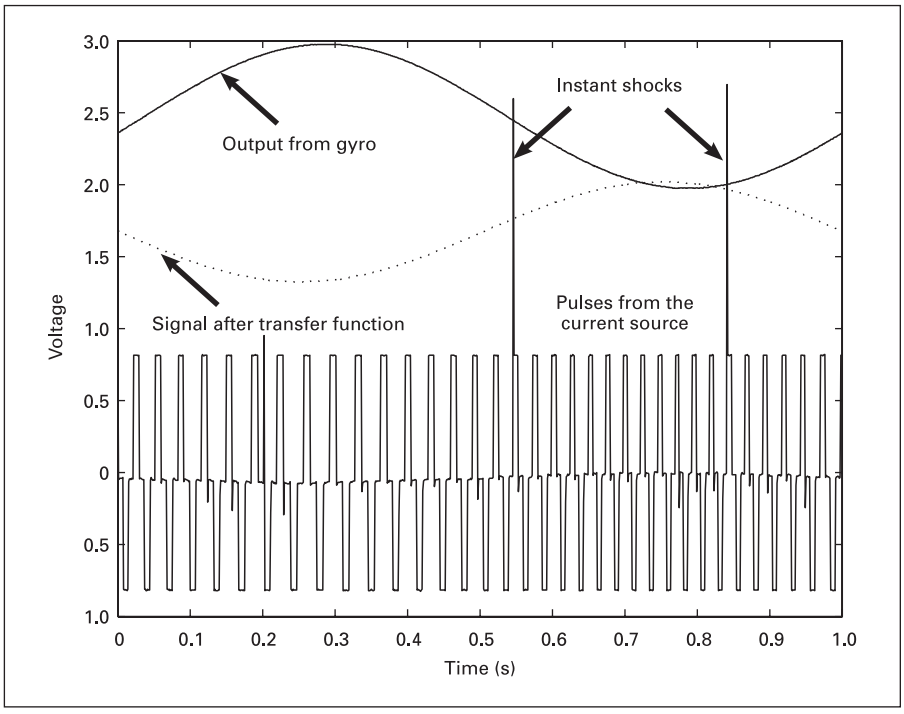

Fig. 5. Electronic evaluation of the vestibular prosthesis. The solid line shows the output of the MEMS gyroscope. The dotted line shows the output of the pulse generator. The pulses are the current source's output, corresponding to the output of the pulse generator (note the greater inter-pulse interval between 0.2 and 0.3 s than between 0.7 and 0.8 s).

function unit and a voltage-to-frequency converter. The current source includes Smith triggers, analog switches and a current mirror. Two 9-volt batteries are used as a power supply for the prototype circuitry and the sensor. Nine potentiometers are utilized to adjust for the resistance parameters, including four time constants in the transfer function (τ_1, τ_2, τ_A, and τ_L), the gain of the transfer function, spontaneous firing rate, pulse amplitude, and duration of both positive and negative phases for the biphasic pulses.

Electronic Evaluation

We have evaluated electronic performance of the vestibular prosthesis prototype against the experimentally obtained results in a squirrel monkey model [Fernandez and Goldberg, 1971]. In their experiment, the animal was mounted in a structure so that the center of the head was coincident with the axis of rotation and the horizontal canal was in the horizontal plane. Sinusoidal rotations with a frequency of 0.1–8 Hz were sequentially applied and responses of the vestibular nerve in terms of the firing rate were monitored and recorded. In our experiment, the prosthesis prototype was placed on a rate table, moving under the same rotational conditions as those reported in Fernandez and Goldberg [1971].

Figure 5 shows a segment of the prosthesis response to inertial stimuli in real time. The continuous line (top trace) is the output of the sensing unit (gyroscope), which accurately reflects the sinusoidal rotation input of the rate table. In this example, the rotation input frequency is 1 Hz and acceleration amplitude is 250°/s^2. The dotted line (second trace) is the analog signal reflecting the output of the transfer function in the pulse generator. The value of this analog signal is used to generate a corresponding pulse rate. Note the apparent phase difference between the gyroscope's output and the pulse generator's output. In this example, the biphasic current pulses generated by the prosthesis dynamically varied from a maximum of 50 spikes/s to a minimum of 30 spikes/s, with a spontaneous rate of 40 spikes/s. We should note that both the spontaneous firing rate and the sensitivity (setting the maximum and the minimum firing rates) can be easily adjusted, should this adjustment be needed to accommodate individual differences. Finally, occasional instant shocks on top of the pulses may occur as a result of conversion of a digital signal to an analog signal. While adding a capacitor parallel to the load can minimize the potential effect of such shocks on the electrode and tissue, more sophisticated circuit design may be required to eliminate them.

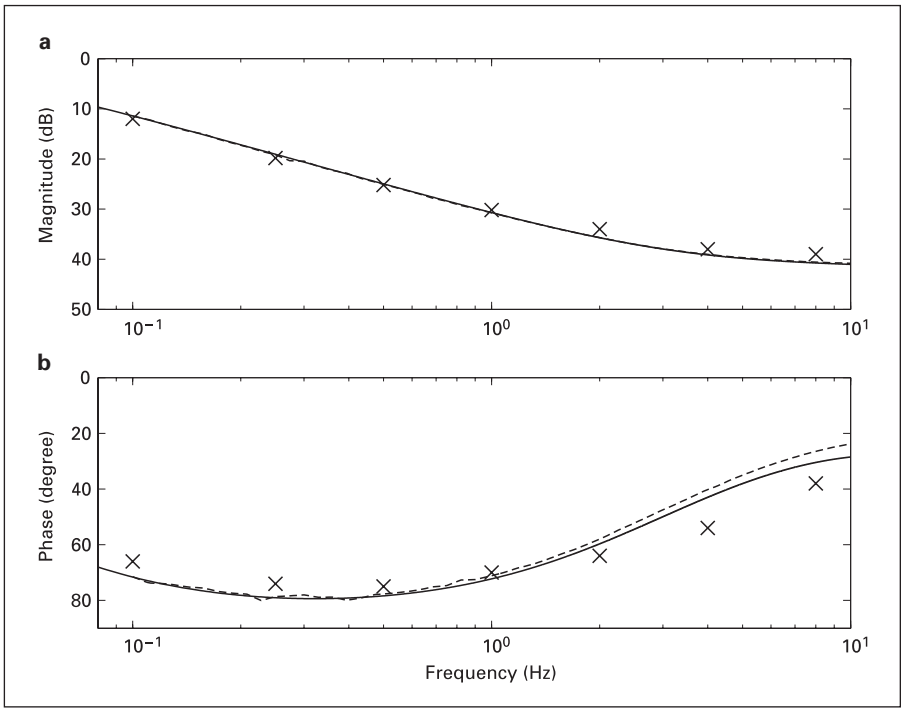

Fig. 6. Magnitude (**a**) and phase (**b**) responses to a sinusoidal stimulus from the actual vestibular nerve fibers in squirrel monkeys [Fernandez and Goldberg, 1971] (crosses), the mathematical model prediction (dashed lines), and the measured output of the present prototype (solid lines). The dashed line is not visible in the magnitude response because the mathematical model prediction totally overlaps with the prototype output.

Figure 6 compares the magnitude (panel a) and phase (panel b) responses for the experimentally obtained data in squirrel monkeys [Fernandez and Goldberg, 1971] (symbols), the mathematical model prediction (dashed lines), and the output of the vestibular prosthesis prototype (solid lines). The dashed line in the magnitude response is not visible because the model prediction is virtually identical to the prototype's output. A comparison is performed for the harmonic angular acceleration with frequencies between 0.1 and 8 Hz. The gain response matches closely for all three sets of data, but the phase response differs slightly, particularly at higher frequencies, reaching 5 degrees between the physiological data and the prototype output at 8 Hz, and 12 degrees between that physiological data and the model prediction at the same frequency. Higher-order models or even nonlinearities simulating the biomechanics of the vestibular end-organ are required to remove this phase difference.

Future Direction

This paper describes the design, implementation and evaluation of an electronic prosthesis mimicking the dynamic function of a unilateral semicircular canal. The encouraging preliminary results have demonstrated the technical feasibility of combining MEMS gyroscopes and analog circuits to reproduce a natural vestibular system's dynamic response to unilateral rotational movement.

The present architecture enables the use of the surface mount hybrid techniques, which can reduce the size of the overall system and potentially implement them on a single chip. Power consumption can also be reduced using the custom-integrated MEMS gyroscope and low-power analog circuitry. Figure 7 shows the conceptual design of a totally implantable version for the next generation of the vestibular prosthesis. A three-axis MEMS gyroscope will be integrated with control and signal conditional electronics on a silicon substrate encapsulated in a vacuum environment (panel a). The same silicon structure will support a stimulating electrode at each end and provide multiple feedthroughs (panel b). Wireless communication capabilities, wireless gain adjustment capabilities, and wireless power supply will be integrated and housed in a glass capsule. The glass capsule will be electrostatically bonded to the substrate to provide hermetic sealing for protection of the receiver circuitry, sensor, and hybrid elements from body fluids.

We should also note that successful implementation of the vestibular prosthesis not only requires innovative engineering solutions but also novel surgical approaches.

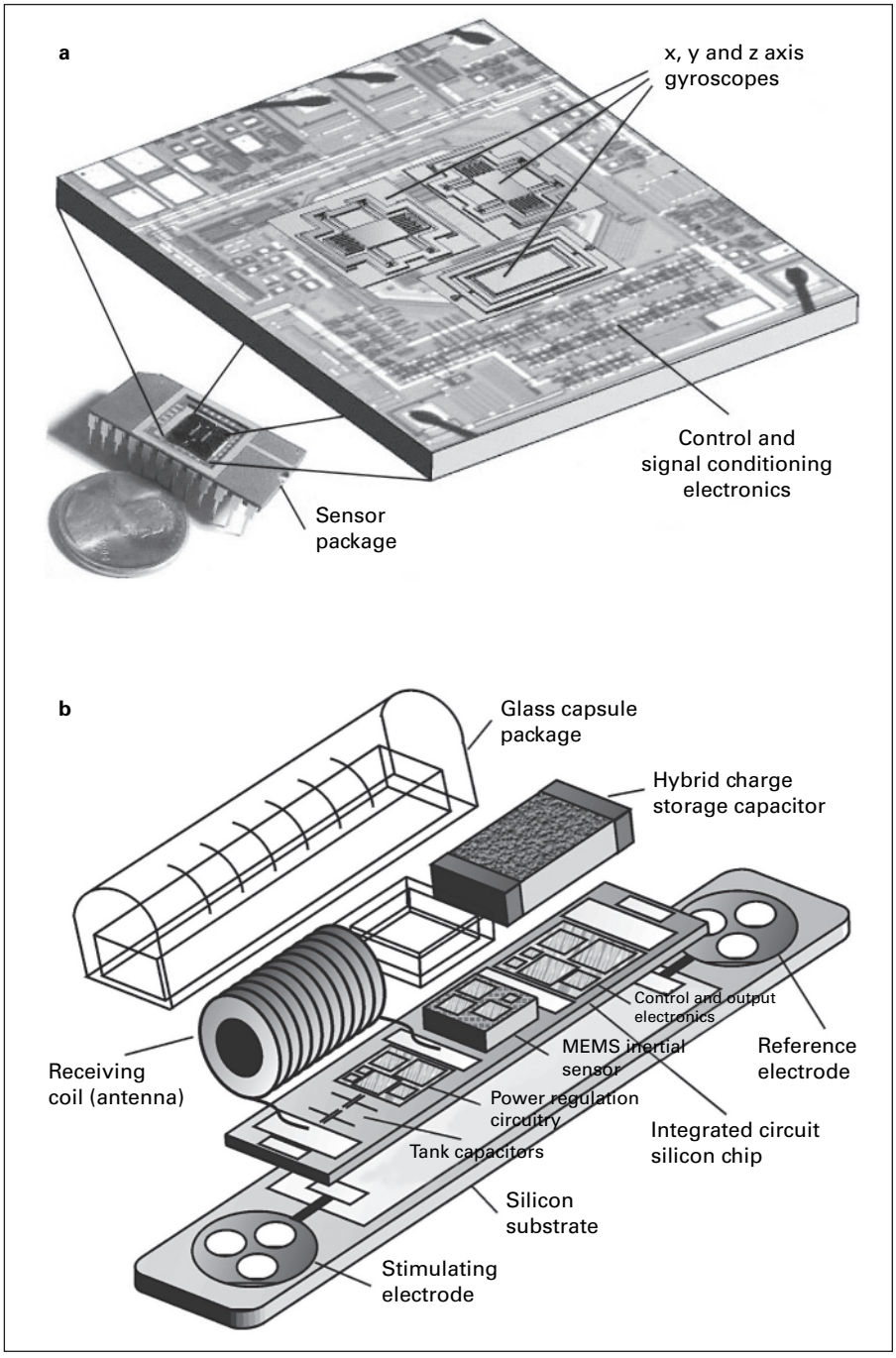

Fig. 7. a Conceptual illustration of the final inertial measurement unit with integrated electronics. **b** Structure of the totally implantable vestibular prosthesis showing the silicon substrate, receiver circuitry, 6-DOF inertial sensors, vacuum packaging cup, and glass capsule.

The implantation procedures and interface with vestibular nerves should minimize the risk of injury to and stimulation of the adjacent facial nerves. In addition, vestibular implantation should not interfere with hearing. An important next step is to demonstrate both the technical and surgical feasibilities of the present vestibular prosthesis prototype in a live animal model.

Acknowledgments

The authors would like to acknowledge Cenk Acar for his contribution in the development of the MEMS gyroscope and Jiayin Liu for her work on the implementation of the pulse generator and current source. We thank Hongbin Chen, Abby Copeland, and two anonymous reviewers for their helpful comments on an earlier version of the manuscript. This project was partially supported by NSF CAREER award CMS-0449442 and NIH RO1 DC002267.

References

Benson AJ, Hutt EC, Brown SF: Thresholds for the perception of whole body angular movement about a vertical axis. Aviat Space Environ Med 1989;60:205–213.

Curthoys IS: The response of primary horizontal semicircular canal neurons in the rat and guinea pig to angular acceleration. Exp Brain Res 1982;47:286–294.

Della Santina CC, Migliaccio AA, Patel AH: Electrical stimulation to restore vestibular function – development of a 3-D vestibular prosthesis. Proc 27th Annu IEEE Eng Med Biol Conf, Shanghai, September 2005.

Fernandez C, Goldberg JM: Physiology of peripheral neurons innervating semicircular canals of the squirrel monkey. II. Response to sinusoidal stimulation and dynamics of peripheral vestibular system. J Neurophysiol 1971;34:661–675.

Gauchard GC, Gangloff P, Jeandel C, Perrin PP: Physical activity improves gaze and posture control in the elderly. Neurosci Res 2003;45:409–417.

Goldberg JM, Fernandez C: Physiology of peripheral neurons innervating semicircular canals of the squirrel monkey. I. Resting discharge and response to constant angular accelerations. J Neurophysiol 1971;34:635–660.

Goldberg JM, Fernandez C: Vestibular mechanisms. Annu Rev Physiol 1975;37:129–162.

Gong W, Merfeld DM: Prototype neural semicircular canal prosthesis using patterned electrical stimulation. Ann Biomed Eng 2000;28:572–581.

Gong W, Merfeld DM: System design and performance of a unilateral horizontal semicircular canal prosthesis. IEEE Trans Biomed Eng 2002;49:175–181.

Greiff P, Boxenhorn B, King T, Niles L: Silicon monolithic micromechanical gyroscope. Tech Dig 6th Int Conf Solid-State Sensors Actuators (Transducers '91), San Francisco, June 1991.

Groen JJ: The semicircular canal system of the organs of equilibrium. I. Phys Med Biol 1956;1:103–117.

Highstein SM, Rabbitt RD, Holstein GR, Boyle RD: Determinants of spatial and temporal coding by semicircular canal afferents. J Neurophysiol 2005;93:2359–2370.

Lewis RF, Gong W, Ramsey M, Minor L, Boyle R, Merfeld DM: Vestibular adaptation studied with a prosthetic semicircular canal. J Vestib Res 2002;12:87–94.

Liu J, Shkel AM, Nie K, Zeng FG: Circuits with adjustable parameters mimicking the function of the natural vestibular end-organ. Proc 1st Int IEEE EMBS Conf Neural Eng, Capri Island, March 2003.

McCreery DB, Agnew WF, Yuen TG, Bullara L: Charge density and charge per phase as cofactors in neural injury induced by electrical stimulation. IEEE Trans Biomed Eng 1990;37:996–1001.

Minor LB: Physiological principles of vestibular function on earth and in space. Otolaryngol Head Neck Surg 1998;118:S5–S15.

Minor LB: Intratympanic gentamicin for control of vertigo in Meniere's disease: vestibular signs that specify completion of therapy. Am J Otol 1999;20:209–219.

Montandon A: A new technique for vestibular investigation. Acta Otolaryngol 1954;39:594.

Patla AE: Strategies for dynamic stability during adaptive human locomotion. IEEE Eng Med Biol Mag 2003;22:48–52.

Rubinstein JT, Della Santina CC: Development of a biophysical model for vestibular prosthesis research. J Vestib Res 2002;12:69–76.

Scheiner A, Mortimer JT, Roessmann U: Imbalanced biphasic electrical stimulation: muscle tissue damage. Ann Biomed Eng 1990;18:407–425.

Shkel AM: Micromachined gyroscopes: challenges, design solutions, and opportunities. SPIE Annu Int Symp Smart Structures Materials, Newport Beach, March 2001.

Shkel AM, Acar C, Painter C: Two types of micromachined vibratory gyroscopes. Int IEEE Sensors Conf, Irvine, 2005.

Shkel AM, Howe RT: Micro-Machined Angle-Measuring Gyroscope. Oakland, University of California Regents, 2002.

Steinhausen W: Über den Nachweis der Bewegung der Cupula in der intakten Bogengangsampulle des Labyrinthes bei der natürlichen rotatorischen und calorischen Reizung. Arch Ges Physiol 1931;228:322–328.

von Egmond AA, Groen J, Jongkees LBW: The mechanics of the semicircular canal. J Physiol 1949;110:1–17.

Wall C 3rd, Merfeld DM, Rauch SD, Black FO: Vestibular prostheses: the engineering and biomedical issues. J Vestib Res 2002;12:95–113.

Weiland JD, Liu W, Humayun MS: Retinal prosthesis. Annu Rev Biomed Eng 2005;7:361–401.

Zeng FG: Trends in cochlear implants. Trends Amplif 2004;8:1–34.

Zeng FG, Galvin JJ: Amplitude mapping and phoneme recognition in cochlear implant listeners. Ear Hear 1999;20:60–74.